Syntheses, Properties, and X-ray Crystal Structures of 17-Electron, Tris(pyrazolyl)borate Compounds of the Types $TpM(CO)_2L$, $Tp^*M(CO)_2L$, and $Tp'M(CO)_2L$ (M = Cr, Mo; Tp = Hydridotris(pyrazolyl)borate, Tp* = Hydridotris(3,5-dimethylpyrazolyl)borate, Tp' = Tetrakis(pyrazolyl)borate; L = CO, Tertiary Phosphines): Synthesis and Crystal Structure of the Alkyl Compound $TpMo(CO)_3CH_2CN$

Joseph H. MacNeil, Aleksander W. Roszak, and Michael C. Baird*

Department of Chemistry, Queen's University, Kingston, Ontario, Canada K7L 3N6

Keith F. Preston†

Steacie Institute of Molecular Sciences, National Research Council, Ottawa, Ontario, Canada K1A 0R9

Arnold L. Rheingold

Department of Chemistry, University of Delaware, Newark, Delaware 19716

Received August 31, 1993®

A series of six-coordinated, 17-electron compounds $TpM(CO)_2L$, $Tp^*M(CO)_2L$, and $Tp'M(CO)_2L$ (M = Cr, Mo; Tp = hydridotris(pyrazolyl)borate, Tp* = hydridotris(3,5-dimethylpyrazolyl)borate, Tp' = tetrakis(pyrazolyl)borate; L = CO, tertiary phosphines), most of them new, has been synthesized and characterized by IR, ^1H NMR, and EPR spectroscopy, cyclic voltammetry, and X-ray crystallography. Formation of the substituted compounds by reactions of the tricarbonyls with phosphines is influenced considerably by steric factors and is complicated by disproportionation and formation of hydrides. All of the tricarbonyl compounds exhibit dynamic Jahn-Teller distortions, the compounds $TpM(CO)_3$ and $Tp^*M(CO)_3$ being EPR-silent except in frozen solutions below 77 K, where the orbital degeneracies are split by the glassy solvent matrices. In contrast, EPR spectra of $Tp'M(CO)_3$ (C_s symmetry or lower) and of the phosphine-substituted compounds are observable at much higher temperatures. Comparisons of the X-ray crystal structures of $Tp'Cr(CO)_3$ and its 18-electron analogue $Tp'Mn(CO)_3$ show that the former exhibits a significant Jahn–Teller distortion in the solid state (OC–Cr–CO bond angles 84.2(2), 85.2(2), and 93.6(2)), while the X-ray crystal structure of $TpMo(CO)_2(PEt_2Ph)$ shows that this compound exhibits the same type of contracted OC–metal–CO bond angle (80.0(1)°) observed previously for the analogous 17-electron compounds η^5-$C_5H_5Cr(CO)_2(PPh_3)$ and η^5-$C_5Me_5Cr(CO)_2(PMe_3)$. The compound $TpMo(CO)_3CH_2CN$ is the first of this class of seven-coordinated alkyl compounds to be reported, and exhibits a "four-legged piano stool" structure. Crystal data for $Tp'Cr(CO)_3$: $P2_1/n$, $Z = 4$ ($a = 8.0381(2)$ Å, $b = 17.192(5)$ Å, $c = 13.089(3)$ Å, $\beta = 95.72(2)°$, and $V = 1800.0$ Å^3, $R_F = 4.8\%$ and $R_{wF} = 5.8\%$). Crystal data for $Tp'Mn(CO)_3$: $P2_1/n$, $Z = 4$ ($a = 13.041(2)$ Å, $b = 17.031(3)$ Å, $c = 8.069(1)$ Å, $\beta = 96.08(1)°$, and $V = 1782.1$ Å^3, $R_F = 4.8\%$ and $R_{wF} = 5.2\%$). Crystal data for $TpMo(CO)_2(PEt_2Ph)$: Cc, $Z = 4$ ($a = 16.097(6)$ Å, $b = 10.160(5)$ Å, $c = 15.444(4)$ Å, $\beta = 108.16(3)°$, and $V = 2400.0$ Å^3, $R_F = 5.1\%$ and $R_{wF} = 5.9\%$). The compound $TpMo(CO)_3$ reacts with $BrCH_2CN$ to form the alkyl derivative $TpMo(CO)_3CH_2CN$, the first of this type known. Crystal data for $TpMo(CO)_3CH_2CN$: $P\bar{1}$, $Z = 2$ ($a = 9.358(2)$ Å, $b = 10.121(2)$ Å, $c = 10.328(4)$ Å, $\alpha = 110.81(3)°$, $\beta = 93.17(3)°$, $\gamma = 105.14(2)°$, and $V = 870.70$ Å^3, $R_F = 4.5\%$ and $R_{wF} = 5.1\%$).

Interest in the chemistry of 17-electron, organotransition metal compounds has grown rapidly in recent years, in part because electronic unsaturation in such molecules leads to significant departures from the structures and chemical reactivities of the corresponding 18-electron, electronically saturated compounds.[1] Thus there is now a very extensive literature concerning the chemistry and the electronic structures of 17-electron complexes, such as $V(CO)_6$,[2] η^5-$C_5R_5Cr(CO)_3$ (R = H, Me, Ph),[3] and [Fe-

† NRCC No. 37206.

® Abstract published in *Advance ACS Abstracts*, October 15, 1993.

(1) (a) Baird, M. C. *Chem. Rev.* **1988**, *88*, 1217. (b) Stiegman, A. E.; Tyler, D. R. *Comments Inorg. Chem.* **1986**, *5*, 215. (c) Kochi, J. K. *Organometallic Reaction Mechanisms and Catalysis*; Academic Press: New York, 1978. (d) Brown, T. L. *Ann. N.Y. Acad. Sci.* **1980**, *330*, 80. (e) Kochi, J. K. *J. Organomet. Chem.* **1986**, *300*, 139. (f) Trogler, W. C., Ed. *Organometallic Radical Processes*; Journal of Organometallic Chemistry Library 22; Elsevier: Berlin, 1990.

0276-7333/93/2312-4402$04.00/0

$(CO)_3(PPh_3)_2]^+$,[4] which are all Jahn–Teller molecules since orbitally degenerate ground states would pertain if the complexes were to assume the ideal structures of their 18-electron analogues, $Cr(CO)_6$ (O_h), η^5-$C_5R_5Mn(CO)_3$ (local C_{3v}), and $Fe(CO)_3(PPh_3)_2$ (local D_{3h}), respectively. Indeed, all have been found to undergo either dynamic Jahn–Teller distortions, in which case low temperatures are required to observe the EPR spectra, or significant static distortions.

An apparent anomaly in this pattern of findings was a report that the 17-electron compound $TpMo(CO)_3$ (Tp = hydridotris(pyrazolyl)borate, i.e. **I** with R = H) assumes

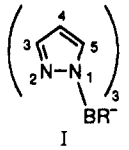

I

a structure which possesses local C_{3v} symmetry about the molybdenum atom.[5a,b] While subtle or dynamic Jahn–Teller distortions might reasonably apply, inconsistent with these possible rationalizations was the observation of a well-resolved, nearly isotropic EPR spectrum in frozen THF at 90 K.

To resolve this anomaly, we have investigated the electronic structures of a series of tris(pyrazolyl)borate derivatives of chromium and molybdenum of the types $TpM(CO)_2L$, $Tp^*M(CO)_2L$, and $Tp'M(CO)_2L$ (Tp^* = hydridotris(3,5-dimethylpyrazolyl)borate, Tp′ = tetrakis(pyrazolyl)borate; L = CO, tertiary phosphines). A communication describing the EPR spectra and discussing the nature of the Jahn–Teller distortions of the tricarbonyl compounds has appeared,[6] and we now present full details concerning the syntheses and spectroscopic and electrochemical properties of the new compounds. We contrast the reactivities of these compounds with those of the analogous 17-electron cyclopentadienyl system, and describe the crystal structures of $Tp'Cr(CO)_3$, $TpMo(CO)_2PEt_2Ph$ and, for purposes of comparion, $Tp'Mn(CO)_3$. We also describe the synthesis and crystal structure of the first known alkyl compound of the type $TpMo(CO)_3R$ (R = CH_2CN), prepared via reactions of bromoacetonitrile with both $TpMo(CO)_3$ and $Et_4N[TpMo(CO)_3]$. While this work was in progress, there appeared descriptions of the analogous $TpW(CO)_3$,[7a,b] of the electrochemistry of the compounds $TpM(CO)_3$[7b,c] (M = Cr, Mo, W) and of the crystal structure of $Tp^*Mo(CO)_3$,[7d] as well as comparisons of two isoelectronic, 17-electron systems $TpM(CO)_3$ and η^5-$C_5R_5Cr(CO)_3$ (R = H, Me, Ph).[7b,c]

Experimental Section

Syntheses were carried out under purified nitrogen in dried, deaerated solvents, utilizing normal Schlenk techniques and a Vacuum Atmospheres glovebox equipped with a Dritrain. IR and ^1H NMR experiments were carried out on Bruker IFS-85 FT-IR and AC 200 NMR spectrometers, respectively. EPR spectra were recorded on a Varian E12 spectrometer equipped with a Bruker ER035M gaussmeter for magnetic field measurements and a Systron-Donner microwave frequency counter. A small liquid nitrogen dewar positioned samples at the center of the resonant rectangular cavity for spectra run at 77 K. Temperature control in the range 4–100 K was achieved with an Oxford instruments liquid helium cryostat, while a gaseous nitrogen cryostat was used for variable temperature studies from 90 to 300 K.

X-ray crystallographic determinations of $Tp'Mn(CO)_3$, $TpMo(CO)_2(PEt_2Ph)$, and $TpMo(CO)_3CH_2CN$ were carried out at Queen's University on an Enraf-Nonius CAD-4 diffractometer using Mo Kα graphite-monochromated X-ray radiation. Structures were solved and refined by direct methods with the XTAL 3.0 program package[8] on a Sun SPARCstation 1. For each compound, an initial scan of the crystal located and centered 25 reflections from which the unit cell and orientation matrix were determined. This list was updated to obtain a refined set of unit cell parameters. An $\omega/2\theta$ data collection was conducted at room temperature, with intensity standards being recorded every 250 reflections and orientation reflections being measured every 7200 s. No significant decay or motion of the crystal was observed throughout the duration of the experiment. The data were corrected for Lorentz and polarization effects; absorption corrections were not applied. A direct methods solution revealed the location of the metal atom position; subsequent Fourier synthesis iterations led to satisfactory location of the remaining non-hydrogen atoms. The solution was refined isotropically, following which the positions of the hydrogen atoms were calculated and inserted with the isotropic temperature factors of their parent atoms.

The X-ray structure determination of $Tp'Cr(CO)_3$ was carried out at the University of Delaware on a Siemens P4 diffractometer

(2) (a) Connelly, N. G. In *Comprehensive Organometallic Chemistry*; Wilkinson, G., Stone, F. G. A., Abel, E. W., Eds.; Pergamon Press: London, 1982; Chapter 24.2. (b) Ishikawa, Y.; Hackett, P. A.; Rayner, D. M. *J. Am. Chem. Soc.* **1987**, *109*, 6644. (c) Jones, L. H.; McDowell, R. S.; Goldblatt, M. *Inorg. Chem.* **1969**, *8*, 2349. (d) Holland, G. F.; Manning, M. C.; Ellis, D. E.; Trogler, W. C. *J. Am. Chem. Soc.* **1983**, *105*, 2308. (e) Devore, T. C.; Franzen, H. F. *Inorg. Chem.* **1976**, *15*, 1318. (f) Ford, T. A.; Huber, H.; Klotzbucher, W.; Moskovits, M. *Inorg. Chem.* **1976**, *15*, 1666. (g) Bellard, S.; Rubinson, K. A.; Sheldrick, G. M. *Acta Crystallogr., Sect. B* **1979**, *35*, 271. (h) Schmidling, D. G. *J. Mol. Struct.* **1975**, *24*, 1. (i) Bernier, J. C.; Kahn, O. *Chem. Phys. Lett.* **1973**, *19*, 414. (j) Barton, T. J.; Grinter, R.; Thomson, A. J. *J. Chem. Soc., Dalton Trans.* **1978**, 608. (k) Calderazzo, F.; Cini, R.; Corradini, P.; Ercoli, R.; Natta, G. *Chem. Ind.* **1960**, 500. (l) Calderazzo, F.; Cini, R.; Ercoli, R. *Chem. Ind.* **1960**, 934. (m) Pratt, D. W.; Myers, R. J. *J. Am. Chem. Soc.* **1967**, *89*, 6470. (n) Rubinson, K. A. *J. Am. Chem. Soc.* **1976**, *98*, 5188. (o) Boyer, M. P.; LePage, Y.; Morton, J. R.; Preston, K. F.; Vuolle, M. *Can. J. Spectrosc.* **1981**, *26*, 181. (p) Ammeter, J. H.; Zoller, L.; Bachmann, J.; Baltzer, P.; Gamp, E.; Bucher, R.; Deiss, E. *Helv. Chim. Acta* **1981**, *64*, 1063. (q) Bratt, S. W.; Kassyk, A.; Perutz, R. N.; Symons, M. C. R. *J. Am. Chem. Soc.* **1982**, *104*, 490. (r) McCall, J. M.; Morton, J. R.; Preston, K. F. *Organometallics* **1985**, *4*, 1272. (s) McCall, J. M.; Morton, J. R.; Preston, K. F. *J. Magn. Reson.* **1985**, *64*, 414.

(3) (a) Cooley, N. A.; Watson, K. A.; Fortier, S.; Baird, M. C. *Organometallics* **1986**, *5*, 2563. (b) McLain, S. J. *J. Am. Chem. Soc.* **1988**, *110*, 643. (c) Krusic, P. J.; McLain, S. J.; Morton, J. R.; Preston, K. F.; LePage, Y. *J. Magn. Reson.* **1987**, *74*, 72. (d) Morton, J. R.; Preston, K. F.; Cooley, N. A.; Baird, M. C.; Krusic, P. J.; McLain, S. J. *J. Chem. Soc., Faraday Trans.* **1987**, *83*, 3535. (e) Jaeger, T. J.; Baird, M. C. *Organometallics* **1988**, *7*, 2074. (f) Fortier, S.; Baird, M. C.; Preston, K. F.; Morton, J. R.; Ziegler, T.; Jaeger, T. J.; Watkins, W. C.; MacNeil, J. H.; Watson, K. A.; Hensel, K.; LePage, Y.; Charland, J.-P.; Williams, A. J. *J. Am. Chem. Soc.* **1991**, *113*, 542. (g) Cooley, N. A.; Baird, M. C.; Morton, J. R.; Preston, K. F.; LePage, Y. *J. Magn. Reson.* **1988**, *76*, 325. (h) O'Callaghan, K. A. E.; Brown, S. J.; Page, J. A.; Baird, M. C.; Richards, T. C.; Geiger, W. E. *Organometallics* **1991**, *10*, 3119. (i) Hoobler, R. J.; Marc, A. H.; Dillard, M. M.; Castellani, M. P.; Rheingold, A. L.; Rieger, A. L.; Rieger, P. H.; Richards, T. C.; Geiger, W. E. *Organometallics* **1993**, *12*, 116. (j) Cooley, N. A.; MacConnachie, P. T. F.; Baird, M. C. *Polyhedron* **1988**, *7*, 1965. (k) Watkins, W. C.; Hensel, K.; Fortier, S.; Macartney, D. H.; Baird, M. C.; McLain, S. J. *Organometallics* **1992**, *11*, 2418. (l) MacConnachie, P. T. F.; Nelson, J. M.; Baird, M. C. *Organometallics* **1992**, *11*, 2521.

(4) MacNeil, J. H.; Chiverton, A. C.; Fortier, S.; Baird, M. C.; Hynes, R. C.; Williams, A. J.; Preston, K. F.; Ziegler, T. *J. Am. Chem. Soc.* **1991**, *113*, 9834.

(5) (a) Shui, K.-B.; Curtis, M. D.; Huffman, J. C. *Organometallics* **1983**, *2*, 936. (b) Curtis, M. D.; Shui, K.-B.; Butler, W. M.; Huffman, J. C. *J. Am. Chem. Soc.* **1986**, *108*, 3335. (c) Shui, K.-B.; Lee, L.-Y.; *J. Organomet. Chem.* **1988**, *348*, 357.

(6) MacNeil, J. H.; Watkins, W. C.; Baird, M. C.; Preston, K. F. *Organometallics* **1992**, *11*, 2761.

(7) (a) Philipp, C. C.; White, P. S.; Templeton, J. L. *Inorg. Chem.* **1992**, *31*, 3825. (b) Bockman, T. M.; Kochi, J. K. *New J. Chem.* **1992**, *16*, 39. (c) Skagestad, V.; Tilset, M. *J. Am. Chem. Soc.* **1993**, *115*, 5077. (d) Protasiewicz, J. D.; Theopold, K. H. *J. Am. Chem. Soc.* **1993**, *115*, 5559.

(8) Hall, S. R., Stewart, J. M., Eds. Xtal User's Reference Manual Version 3.0. Universities of Western Australia and Maryland, 1990.

Table I. Carbonyl Stretching Frequencies (THF)

compd	ν(CO) (cm^{-1})
$TpMn(CO)_3$[a]	2036 (s), 1932 (s)
$Tp'Mn(CO)_3$[a]	2039 (s), 1936 (s)
$TpCr(CO)_3$	2024 (s), 1865 (s, br)
$Tp^*Cr(CO)_3$	2015 (s), 1844 (s, br)
$Tp'Cr(CO)_3$	2026 (s), 1861 (s, br)
$TpMo(CO)_3$	2007 (s), 1873 (s, br)
$TpMo^*(CO)_3$[b]	1997 (s), 1863 (vs)
$Tp'Mo(CO)_3$	2008 (s), 1876 (s, br)
$TpW(CO)_3$[c]	1983 (s), 1854 (s, br)
$TpCr(CO)_2(PMe_3)$	1912 (s), 1757 (s)
$TpCr(CO)_2(PMe_2Ph)$	1915 (s), 1759 (s)
$Tp'Cr(CO)_2(PBu_3)$	1912 (s), 1758 (s)
$TpMo(CO)_2(PMe_3)$	1903 (s), 1767 (s)
$TpMo(CO)_2(PMe_2Ph)$	1905 (s), 1771 (s)
$TpMo(CO)_2(PBu_3)$	1901 (s), 1766 (s)
$TpMo(CO)_2(PEt_2Ph)$	1903 (s), 1770 (s)
$TpMo(CO)_2(PMePh_2)$	1906 (s), 1774 (s)
$TpMo(CO)_2(PEtPh_2)$	1905 (s), 1772 (s)
$Tp'Mo(CO)_2(PMe_3)$	1903 (s), 1772 (s)
$Tp'Mo(CO)_2(PBu_3)$	1903 (s), 1769 (s)
$Tp'Mo(CO)_2(PMe_2Ph)$	1905 (s), 1772 (s)

[a] In MeCN. [b] Reference 5c. [c] Reference 7a.

Table II. ^1H NMR Data ($CDCl_3$)

	chemical shifts (δ)[a]					
compd	H_3, Me_3	H_4	H_5, Me_5	H_3'	H_4'	H_5'
$TpCr(CO)_3$	−8.0	3.03	−15.7			
$Tp^*Cr(CO)_3$	15.8	1.10	26.7			
$Tp'Cr(CO)_3$	−9.4	3.69	−16.0	8.65	7.37	10.04
$TpMo(CO)_3$	−8.0	3.57	−18.3			
$TpMo^*(CO)_3$[a]	18.8	1.45	35.6			
$TpMo'(CO)_3$	−9.7	4.41	−18.0	9.65	8.07	11.77

[a] H_3', H_4', and H_5' are the protons on the uncoordinated pyrazolyl ring.

equipped with Mo Ka radiation. Computations used the SHELXTL PLUS (VMS version) software system (G. Sheldrick, Siemens, Madison, WI).

CV data were obtained with a BAS CV-1B cyclic voltammograph and plotted on a Houston Instruments Omnigraph 100 chart recorder. A glassy carbon working electrode, platinum wire auxiliary electrode, and $Ag^+/AgCl$ reference electrode were used to record all scans. Fresh test solutions were prepared immediately prior to each experiment, and contained 1×10^{-3} M analyte and 0.1 M [n-Bu_4N][BF_4] supporting electrolyte. All reported data are referenced to the ferrocene/ferrocenium couple (Cp_2Fe/Cp_2Fe^+) in the appropriate solvent.[9] Elemental analyses were performed by Canadian Microanalytical Services, Victoria, British Columbia.

Syntheses of $[Cp_2Fe]PF_6$,[10] NaTp,[11a] NaTp',[11a] NaTp*,[11a,b] $TpMn(CO)_3$[11b] $TpMo(CO)_3H$,[12] $TpMo(CO)_3$,[5a,b] and $Tp^*Mo(CO)_3$[5c] were carried out as described previously, the latter two compounds with minor modifications. The published procedures involved oxidation of the corresponding 18-electron, anionic species with ferrocenium ion in THF at room temperature. In our hands, room temperature syntheses of $TpMo(CO)_3$ resulted in the formation of considerable amounts of $TpMo(CO)_3H$,[12] formation of which was readily avoided by cooling the reaction mixture to −40 °C.

Syntheses of the Compounds $LM(CO)_3$ (L = Tp, Tp*, Tp'; M = Cr, Mo). Procedures were essentially as described above for $TpMo(CO)_3$, and IR and NMR data for all of the compounds synthesized are presented in Tables I and II, respectively. In a typical experiment, the starting carbonylate anion was formed by refluxing $Cr(CO)_6$ or $Mo(CO)_6$ with NaTP, NaTp*, or NaTp' in the presence of Et_4NCl and then reacted with an equimolar amount of $[Cp_2Fe]PF_6$ in THF at −40 °C (acetonitrile slush bath). The reactions proceeded from opaque green initial colors to clear orange solutions, generally within 30 min. When the starting materials had been consumed, the reaction mixtures were filtered through Celite to remove the precipitated NEt_4PF_6, following which the THF was removed *in vacuo*. The best method of subsequent purification varied with the different compounds, and will be detailed below.

Table III. Crystallographic Data for $Tp'Cr(CO)_3$

mol formula	$C_{15}H_{12}BCrN_8O_3$
mol wt	415.12
space group	$P2_1/n$ (No. 14)
a (Å)	8.0381(2)
b (Å)	17.192(5)
c (Å)	13.089(3)
β (deg)	95.72(2)
vol (Å^3)	1800.0
Z	4
μ (mm^{-1})	0.671
dens (g cm^{-3})	1.558
T (K)	298
cryst dimens (mm)	0.36 × 0.36 × 0.36
F(000)	844
λ(Mo Kα) (Å)	0.710 732
2θ range scanned (deg)	4.0 → 60.0
(sin θ)/λ max	0.595
h,k,l range obsd	−11 → 11, 0 → 24, 0 → 18
no. of unique reflns	5260
no. of obsd reflns	3201 ($F > 4\sigma F$)

Purification of $TpCr(CO)_3$ proved exceedingly difficult. The most effective method employed was chromatography on silica, initially eluting the ferrocene contaminant with hexanes and then rapid recovering the product with 1:1 CH_2Cl_2–hexanes. The compound was unstable in solution; while an IR spectrum sampled directly from the column eluant indicated the compound was pure, some decomposition was obvious in the time required to pump the product to dryness, even when the solvent was cooled to 273 K. All attempts to crystallize $TpCr(CO)_3$ were unsuccessful as well. Inability to obtain an analytically pure sample was reflected in the elemental analysis results. Anal. Calcd for $C_{12}H_{10}BCrN_6O_3$: C, 41.29; H, 2.89; N, 24.08. Found: C, 38.88; H, 2.91; N, 20.05.

In a procedure similar to that reported for $Tp^*Mo(CO)_3$,[5c] $Tp^*Cr(CO)_3$ was purified by thrice washing the product with small (~5-mL) aliquots of acetonitrile and hexanes and then by drying *in vacuo* for 24 h. Anal. Calcd for $C_{18}H_{22}BCrN_6O_3$: C, 49.90; H, 5.12; N, 19.40. Found: C, 49.78; H, 5.10; N, 19.21.

Reasonable purification of $Tp'Cr(CO)_3$ was achieved by washing the product with hexanes, although recrystallization from MeCN was required to remove all traces of ferrocene. The dark, opaque crystals redissolved to yield yellow solutions with the correct spectroscopic properties and gave an adequate elemental analysis. Anal. Calcd for $C_{16}H_{12}BCrN_8O_3$: C, 43.40; H, 2.91; N, 26.99. Found: C, 43.48; H, 2.93; N, 28.23.

Slow cooling of a concentrated solution of $Tp'Cr(CO)_3$ in acetonitrile proved to be the most effective method of achieving X-ray quality crystals. A dark, cube-shaped crystal was mounted on a glass fiber and found photographically to possess $2/m$ Laue symmetry. A Wyckoff data collection was conducted at room temperature, with intensity standards being recorded every 197 reflections. A summary of experimental conditions is presented in Table III. The data were corrected for Lorentz and polarization effects, but absorption corrections were not required (ψ-scan variation <8%). The chromium atom was located by direct methods. Full-matrix least-squares refinement of positional and anisotropic thermal parameters for all non-hydrogen atoms included 2502 observed reflections. Idealized hydrogen atoms were assigned an isotropic temperature factor 1.2× their parent atoms and were not further refined. In the final cycles of refinement anisotropic temperature factors were employed for all non-hydrogen atoms; 248 variable parameters converged to

(9) (a) Gange, R. R.; Koval, C. A.; Lisensky, G. C. *Inorg. Chem.* **1980**, *19*, 2855. (b) Hershberger, J. W.; Klinger, R. J.; Kochi, J. K. *J. Am. Chem. Soc.* **1982**, *104*, 3034.
(10) Smart, J. C.; Pinsky, B. L. *J. Am. Chem. Soc.* **1980**, *102*, 1009.
(11) (a) Trofimenko, S. *J. Am. Chem. Soc.* **1967**, *89*, 3170. (b) Trofimenko, S. *J. Am. Chem. Soc.* **1969**, *91*, 558.
(12) Curtis, M. D.; Shui, K.-B. *Inorg. Chem.* **1985**, *24*, 1213.

Table IV. Selected Bond Lengths and Angles for Tp'Cr(CO)$_3$ and Tp'Mn(CO)$_3$

Tp'Cr(CO)$_3$		Tp'Mn(CO)$_3$
	a. Bond Lengths (Å)	
2.109(2)	M–N1	2.064(3)
2.051(2)	M–N3	2.052(3)
2.080(3)	M–N5	2.029(3)
1.857(4)	M–C1	1.802(5)
1.914(4)	M–C2	1.806(4)
1.891(3)	M–C3	1.820(5)
1.151(6)	C1–O1	1.139(6)
1.142(4)	C2–O2	1.140(5)
1.140(4)	C3–O3	1.132(6)
	b. Bond Angles (deg)	
85.1(1)	N1–M–N3	84.8(1)
84.3(1)	N1–M–N5	85.7(1)
84.7(1)	N3–M–N5	85.8(1)
84.2(2)	C1–M–C2	89.7(2)
85.2(2)	C1–M–C3	88.5(2)
93.6(2)	C2–M–C3	91.9(2)
179.5(1)	N1–M–C1	177.5(2)
177.4(1)	N3–M–C2	174.4(2)
173.6(1)	N5–M–C3	178.4(2)
176.5(4)	M–C1–O1	178.9(4)
175.5(3)	M–C2–O2	176.4(4)
177.0(3)	M–C3–O3	177.3(4)

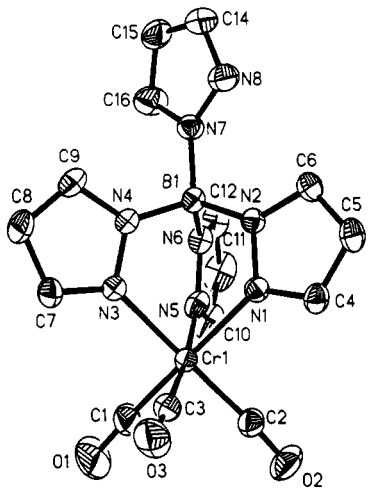

Figure 1. ORTEP plot of Tp'Cr(CO)$_3$.

give disagreement factors R = 4.8% and R_w = 5.8%. The weighting scheme employed was $w^{-1} = \sigma^2(F) + 0.0010(F^2)$. Selected bond lengths and angles are listed in Table IV. An ORTEP structure is presented in Figure 1.

The compound Tp'Mo(CO)$_3$ was freed of ferrocene chromatographically (silica column, hexanes eluant) and then eluted as the pure material with 3:1 hexanes–CH_2Cl_2. It was characterized spectroscopically.

Substitution Reactions of TpM(CO)$_3$, Tp*M(CO)$_3$, and Tp'M(CO)$_3$ with Tertiary Phosphines. Several of the phosphine substitution reactions generated significant amounts of one or more byproducts and/or yielded products which were thermally labile. Thermal decomposition of the starting materials to the corresponding hydrides was a general problem in the cases of slow reactions. Isolation and characterization of many of the phosphine-substituted species was therefore not generally possible, and assignments were based on unambiguously identified compounds. The majority of the reactions were conducted on a scale suitable for monitoring by IR spectroscopy; approximately 300 mg of freshly prepared tricarbonyl compound was reacted with an excess of phosphine in THF, except where otherwise indicated. IR data for the phosphine-substituted complexes are compiled in Table I.

Reaction of TpCr(CO)$_3$ with PMe$_3$. Reaction of TpCr(CO)$_3$ with an 11-fold excess of PMe$_3$ at room temperature proceeded cleanly but slowly; some TpCr(CO)$_3$ was still not consumed after 24 h. Formation of TpCr(CO)$_2$(PMe$_3$) was indicated by the appearance of bands in the IR spectrum at 1912 and 1757 cm^{-1}, and purification was achieved, after removal of the THF, using a silica column. Elimination of the ferrocene generated in the preparation of the parent compound was accomplished by elution of the reaction mixture with hexanes, and isolation of the product as a yellow solid was then realized by elution with a 3:1 hexanes–CH_2Cl_2 mixture followed by removal of solvent. Anal. Calcd for $C_{14}H_{19}BCrN_6O_2P$: C, 42.35; H, 4.82; N, 21.17. Found: C, 42.03; H, 4.99; N, 19.55.

Reaction of TpCr(CO)$_3$ with PMe$_2$Ph. The reaction of TpCr(CO)$_3$ with a 7-fold excess of PMe$_2$Ph also required about 24 h, TpCr(CO)$_2$(PMe$_2$Ph) formation being indicated by the appearance of bands in the IR spectrum at 1915 and 1759 cm^{-1}. The product could not be isolated as pure material.

Reaction of Tp'Cr(CO)$_3$ with PBu$_3$. Reaction with a 3-fold excess of the phosphine proceeded cleanly to completion within 12 h at room temperature, the IR bands of Tp'Cr(CO)$_2$(PBu$_3$) being observed at 1912 and 1758 cm^{-1}.

Reaction of TpMo(CO)$_3$ with PMe$_3$. Reaction of an 8-fold excess of PMe$_3$ proceeded to completion within 10 min of its addition to a THF solution of TpMo(CO)$_3$ cooled to 273 K. By lowering the temperature to 233 K and using only a 2-fold excess of phosphine, the total reaction time was increased to approximately 15 min, affording the opportunity to monitor the reaction more carefully. Accompanying the appearance in the IR spectrum of the carbonyl stretches of TpMo(CO)$_2$(PMe$_3$) at 1903 and 1767 cm^{-1}, a pair of strong bands at 2042 and 1963 cm^{-1} were also observed in the first IR spectrum of the reaction at 233 K. The latter bands were much weaker in spectra of samples taken later in the reaction and had completely disappeared within 25 min. A pair of bands at 1892 and approximately 1758 cm^{-1}, attributable to the anion [TpMo(CO)$_3$]$^-$, were also observed.

Reaction of TpMo(CO)$_3$ with PMe$_2$Ph. A 6-fold aliquot of PMe$_2$Ph reacted to completion in approximately 100 min in a solution allowed to warm very slowly from 233 K, while removal of the cold bath immediately after phosphine addition resulted in all of the tricarbonyl compound being consumed within 1 h. Strong bands at 2041 and 1961 cm^{-1} were observed in the initial IR spectra but had almost disappeared after 1 h in the reaction conducted at lower temperature. The IR bands of TpMo(CO)$_2$(PMe$_2$Ph) at 1905 and 1771 cm^{-1} exhibited weak shoulders on their low frequency side, indicating formation of minor amounts of [TpMo(CO)$_3$]$^-$, and a second pair of peaks, at 1951 and 1867 cm^{-1}, were attributed to the substituted hydride compound TpMo(CO)$_2$(PMe$_2$Ph)H (see below).

The products generated in the warmer reaction were precipitated by the addition of 20 mL of hexanes, following which the solution phase was removed by cannulation and the resulting deep brown solid was dried *in vacuo*. A ^{1}H NMR spectrum of the solid, recorded in $CDCl_3$, clearly exhibited a doublet in the hydride region (δ −4.02, J 70.2 Hz), suggesting that a hydride, presumably TpMo(CO)$_2$(PMe$_2$Ph)H, had formed. Unfortunately, the Tp portion of the spectrum was totally obscured by the phenyl resonances of the PMe$_2$Ph ligand, rendering further assignments impossible.

Reaction of TpMo(CO)$_3$ with PBu$_3$. A 2-fold phosphine excess was added to a solution of TpMo(CO)$_3$, and the reaction mixture was stirred at room temperature for 90 min to achieve complete reaction, as indicated by the appearance of IR carbonyl stretches of TpMo(CO)$_2$(PBu$_3$) at 1904 and 1769 cm^{-1}. Weak bands were also observed at 2042 and 1963 cm^{-1}. Similar results were obtained in toluene and CH_2Cl_2.

Reaction of TpMo(CO)$_3$ with PEt$_2$Ph. A 5-fold excess of PEt$_2$Ph required 3 h at room temperature for the substitution reaction to reach completion, the bands for TpMo(CO)$_2$(PEt$_2$Ph) appearing at 1903 and 1770 cm^{-1}. High frequency bands also appeared at 2040 and 1964 cm^{-1}, as well as evidence for TpMo(CO)$_3$H. At the conclusion of the reaction, the THF solvent was removed *in vacuo* and the product was redissolved to form a saturated CH_2Cl_2 solution; this was syringed onto a silica chromatographic column and evaporated. Ferrocene generated

as a byproduct in the initial preparation of $TpMo(CO)_3$ was first eluted with pure hexanes, then a 4:1 hexanes–CH_2Cl_2 solvent mixture was used to elute $TpMo(CO)_2(PEt_2Ph)$ as an orange-yellow band. The solvent was removed *in vacuo*, and the resultant brown powder was redissolved in acetonitrile to form a saturated solution. Translucent orange crystals were obtained, on cooling to 233 K. Anal. Calcd for $C_{21}H_{25}BMoN_6O_2P$: C, 47.48; H, 4.74; N, 15.82. Found: C, 47.32; H, 4.84; N, 15.66. Crystals prepared in this manner were employed in the X-ray structure determination of $TpMo(CO)_2(PEt_2Ph)$ described below.

Reaction of $TpMo(CO)_3$ with $PMePh_2$. A 6-fold excess of phosphine reacted to yield $TpMo(CO)_2(PMePh_2)$ within 3 h, as indicated by bands at 1903 and 1774 cm^{-1} in the IR spectrum. Slow formation of the tricarbonyl hydride complex was once again apparent, but high frequency peaks were not detectable.

Reaction of $TpMo(CO)_3$ with $PEtPh_2$. This reaction proceeded much more slowly, but after stirring for 24 h at room temperature with a 5-fold phosphine excess, $TpMo(CO)_3$ was almost completely absent from solution. Since the IR bands for $TpMo(CO)_2(PEtPh_2)$, at 1903 and 1774 cm^{-1}, were no longer increasing in intensity, the reaction was terminated. A weak peak was observed at 2039 cm^{-1}, but the most significant product of the reaction was clearly the tricarbonyl hydride, with the bands of $TpMo(CO)_3H$ dominating the IR spectrum of the ultimate product distribution.

Reaction of $TpMo(CO)_3$ with PPh_3. A 5-fold excess of PPh_3 was added to a solution of $TpMo(CO)_3$ in THF, and the reaction mixture was stirred for 48 h; over that period no evidence of phosphine substitution was observed, but the transformation of the tricarbonyl compound to $TpMo(CO)_3H$ was complete. A second solution, again containing a 5-fold excess of PPh_3, was reacted at room temperature for 2 h and then heated to reflux for a further 2 h. While this resulted in total decomposition of $TpMo(CO)_3$, no phosphine-substituted compound could be observed in the IR spectrum. The dark decomposition products were not identified, but solid-state IR spectra, run both as a Nujol mull and in a KBr pellet, indicated a complete lack of carbonyl-containing species. In a third attempt, a 2-fold excess of trimethylamine oxide (Me_3NO) was added to a solution containing a 5-fold excess of PPh_3, in the hope of promoting carbonyl substitution. Addition of the amine oxide caused the solution to quickly darken in color, and IR bands for the $[TpMo(CO)_3]^-$ anion grew in almost immediately; no phosphine-substitution products were ever observed.

Reaction of $Tp'Mo(CO)_3$ with PMe_3. The reaction of a 5-fold excess of PMe_3 proceeded to completion within 15 min as the solution warmed slowly from 233 K, as evidenced by the complete consumption of $Tp'Mo(CO)_3$ and the appearance of carbonyl stretching bands for $Tp'Mo(CO)_2(PMe_3)$ at 1912 and 1757 cm^{-1}. A second product, probably $Tp'Mo(CO)_2(PMe_3)H$, also formed, with IR bands (1951 and 1864 cm^{-1}) of greater intensity than those of $Tp'Mo(CO)_2(PMe_3)$. In a second reaction, the tricarbonyl compound was generated in THF, then pumped dry and dissolved in toluene. A 6-fold excess of PMe_3 was added to the toluene solution and allowed to react at room temperature for 5 min; $Tp'Mo(CO)_2(PMe_3)$ was now the predominant product, although formation of the substituted hydride was still clearly evident. In addition, low frequency shoulders on the IR bands of $Tp'Mo(CO)_2(PMe_3)$ indicated the formation of $[Tp'Mo(CO)_3]^-$ in each of the above reactions.

Reaction of $Tp'Mo(CO)_3$ with PBu_3. Addition of a 4-fold excess of PBu_3 to a solution of the tricarbonyl compound cooled to 233 K resulted in the total consumption of $Tp'Mo(CO)_3$ within 2 h as the solution slowly warmed. IR bands appeared at 1903 and 1769 cm^{-1}, attributed to $Tp'Mo(CO)_2(PBu_3)$, and (more slowly) at 1942 and 1864 cm^{-1}, possibly to be attributed to $TpMo(CO)_2(PMe_2Ph)H$. There also appeared high frequency bands at 2039 and 1962 cm^{-1}; these disappeared over 12 h, apparently accompanied by a concomitant increase in the intensities of the absorptions at 1903 and 1769 cm^{-1}.

Reaction of $Tp'Mo(CO)_3$ with PMe_2Ph. Slow warming from 233 K of a solution of $Tp'Mo(CO)_3$ containing a 2-fold excess of phosphine resulted in clean generation over 4 h of the anticipated substitution product $Tp'Mo(CO)_2(PMe_2Ph)$, as indicated by IR bands at 1905 and 1772 cm^{-1}. No evidence of the phosphine-substituted hydride or the high frequency peaks was observed in this reaction, although very minor quantities of $Tp'Mo(CO)_3H$ did form.

Table V. Crystallographic Data for $TpMo(CO)_2(PEt_2Ph)$

mol formula	$C_{21}H_{25}BMoN_6O_2P$
mol wt	531.19
space group	*Cc* (No. 7)
a (Å)	16.097(6)
b (Å)	10.160(5)
c (Å)	15.444(4)
β (deg)	108.16(3)
vol (Å^3)	2400.0
Z	4
μ (mm^{-1})	0.637
dens (g cm^{-3})	1.470
T (K)	292
cryst dimens (mm)	0.40 × 0.40 × 0.30
F(000)	1084
λ(Mo Kα) (Å)	0.710 732
2θ range scanned (deg)	0 → 50.0
$(\sin\theta)/\lambda$ max	0.595
h,k,l range obsd	0 → 19, 0 → 12, −18 → 17
no. of unique reflns	2108
no. of obsd reflns	1659 ($I > 3\sigma_I$)

Table VI. Selected Bond Lengths and Angles of $TpMo(CO)_2(PEt_2Ph)$

Bond Lengths (Å)			
Mo–N1	2.276(12)	Mo–C1	1.828(2)
Mo–N3	2.221(13)	Mo–C2	1.931(4)
Mo–N5	2.193(13)	C1–O1	1.246(15)
Mo–P	2.485(6)	C2–O2	1.146(11)
Bond Angles (deg)			
N1–Mo–C2	169.1(3)	P–Mo–C2	97.2(2)
N3–Mo–C1	178.3(4)	C1–Mo–C2	80.0(1)
N5–Mo–P	167.8(4)	Mo–C1–O1	172.1(8)
P–Mo–C1	90.2(2)	Mo–C2–O2	176.5(9)

Attempted Reactions of $Tp^*Mo(CO)_3$ with PMe_3 and PPh_3. Attempts to react $Tp^*Mo(CO)_3$ with large excesses of these phosphines were unsuccessful. Neither refluxing in THF and toluene solutions (PPh_3) nor the addition of Me_3NO (PMe_3) yielded any indication of phosphine-substituted species in the IR spectra. Interestingly, $Tp^*Mo(CO)_3$ appeared to be much more robust than its $TpMo(CO)_3$ analogue, as it survived several hours of refluxing in THF and did not decompose in the presence of amine oxide.

Crystal Structure Determination of $TpMo(CO)_2(PEt_2Ph)$. X-ray quality single crystals of $TpMo(CO)_2(PEt_2Ph)$ were grown by slowly cooling saturated acetonitrile solutions to 233 K. A deep orange crystal was mounted on a glass fiber and sealed with a capillary and epoxy. Full-matrix least-squares refinement of positional and thermal parameters for all non-hydrogen atoms included 1659 observed reflections. In the final cycles of refinement anisotropic temperature factors were employed; 289 variable parameters converged to give disagreement factors R = 5.1% and R_w = 5.9%. The weighting scheme employed was calculated with the program REGWT from the XTAL 3.0 crystallography software[8] to best fit the observed reflections. A complete summary of experimental conditions is presented in Table V, and selected bond distances and angles are listed in Table VI. An ORTEP structure is presented in Figure 2.

Synthesis of $Tp'Mn(CO)_3$. A 1.04-g (3.78-mmol) sample of $Mn(CO)_5Br$ and 1.42 g (4.70 mmol) of $NaTp'$ were stirred at room temperature in DMF one 1 h and then warmed gently to 40 °C for a further 20 min. At this point 200 mL of deaerated, ice-cold water was added to the clear orange solution, generating an opaque yellow suspension. The product was extracted with three fractions of CH_2Cl_2 and pumped to dryness, leaving an orange solid in nearly quantatative yield. IR (MeCN): ν_{CO} 2039 (s), 1936 cm^{-1} (s, br). ^1H NMR ($CDCl_3$): δ 7.95 (1 H), 7.92 (4 H), 7.74 (3 H), 6.59 (1 H), 6.24 (3 H).

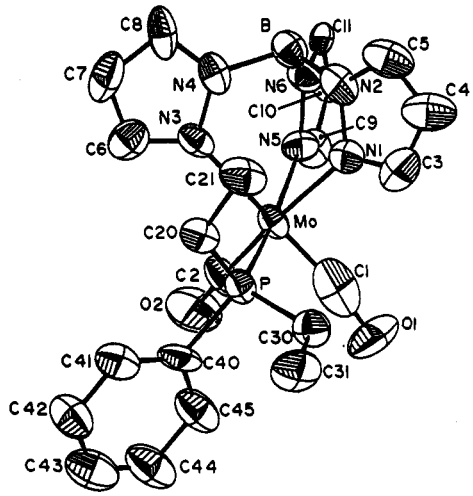

Figure 2. ORTEP plot of $TpMo(CO)_2(PEt_2Ph)$.

Table VII. Crystallographic Data for Tp'Mn(CO)$_3$

mol formula	$C_{15}H_{12}BMnN_8O_3$
mol wt	418.06
space group	$P2_1/n$ (No. 14)
a (Å)	13.041(2)
b (Å)	17.031(3)
c (Å)	8.069(1)
β (deg)	96.08(1)
vol (Å^3)	1782.1
Z	4
μ (mm^{-1})	0.816
dens (g cm^{-3})	1.558
T (K)	292
cryst dimens (mm)	0.50 × 0.40 × 0.35
F(000)	848
λ(Mo Kα) (Å)	0.710 732
2θ range scanned (deg)	1.0 → 50.0
(sin θ)/λ max	0.595
h,k,l range obsd	0 → 15, 0 → 20, −9 → 9
no. of unique reflns	3092
no. of obsd reflns	2502 ($I > 3\sigma I$)

Crystal Structure Determination of Tp'Mn(CO)$_3$. Slow cooling of a concentrated solution of $Tp'Mn(CO)_3$ in acetonitrile proved to be the most effective method of achieving X-ray quality crystals. An orange, transparent crystal of blocklike external form was mounted on a glass fiber and sealed within a capillary with epoxy. Full-matrix least-squares refinement of positional and thermal parameters for all non-hydrogen atoms included 2502 observed reflections. In the final cycles of refinement anisotropic temperature factors were employed; 248 variable parameters converged to give disagreement factors R = 4.8% and R_w = 5.2%. The weighting scheme employed was $\sum_h w(|F_o| - |F_c|)^2$, where $w^{-1} = \sigma F_o$. A complete summary of experimental conditions is presented in Table VII, and selected bond distances and angles are listed in Table IV. An ORTEP structure is illustrated in Figure 3.

Synthesis of TpMo(CO)$_3$CH$_2$CN. Reaction of 0.343 g (0.660 mmol) of $[NEt_4][TpMo(CO)_3]$ with 0.22 mL (3.2 mmol) of bromoacetonitrile at room temperature in CH_2Cl_2 proceeded cleanly to completion within 90 min. The solvent was removed *in vacuo*, and the resulting solid was extracted with three 20-mL portions of toluene. The volume of the combined toluene solutions was reduced by half *in vacuo*, and approximately 25 mL of hexanes was added, causing $TpMo(CO)_3CH_2CN$ to precipitate. The remaining solution was cannulated off, and the solid was pumped to dryness once again. A concentrated solution was prepared in CH_3CN and cooled to 233 K for 3 days, yielding clear yellow single crystals of X-ray quality. IR (CH_2Cl_2): ν(CO) 2025 (s), 1942 (s), 1927 cm^{-1} (m, sh). IR (toluene): ν(CO) 2024 (s), 1944 (s), 1921 cm^{-1} (m). ^{1}H NMR ($CDCl_3$): δ 8.12 (d, J_{H-H} 2.17 Hz, 3 H), 7.67 (d, J_{H-H} 2.27 Hz, 3 H), 6.31 (t, J_{H-H} 2.27 Hz, 3 H), 1.84 (s, 2 H). Anal. Calcd for $C_{14}H_{12}BMoN_7O_3$: C, 38.36; H, 2.79; N, 22.64. Found: C, 38.25; H, 2.82; N, 22.74.

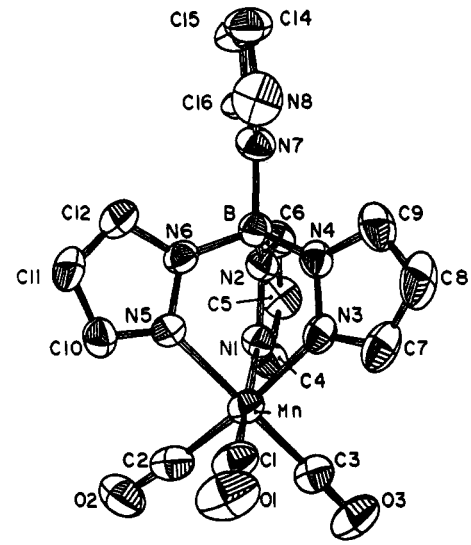

Figure 3. ORTEP plot of $Tp'Mn(CO)_3$.

The compound $TpMo(CO)_3CH_2CN$ can also be synthesized in good yield from reaction of $TpMo(CO)_3$ and $BrCH_2CN$ in CH_2Cl_2, in which solvent IR bands for both $TpMo(CO)_3Br$ and $TpMo(CO)_3CH_2CN$ appear within 1 h. After 24 h, the alkyl compound had totally decomposed, leaving only $TpMo(CO)_3Br$. An NMR spectrum of a reaction run in $CDCl_3$ exhibited the resonances of both $TpMo(CO)_3Br$ and $TpMo(CO)_3CH_2CN$. Reaction was complete within 90 min, and integrations suggested approximately 50% more of the bromo compound had been formed during that time.

Crystal Structure of TpMo(CO)$_3$CH$_2$CN. A clear yellow crystal grown from a saturated CH_3CN solution at 233 K was secured to the end of a glass fiber with epoxy and then sealed within a nitrogen atmosphere by capping both crystal and fiber with a capillary. Additional epoxy was applied to the base of the capillary to ensure an airtight seal, and the entire assembly was removed from the glovebox, inserted into a goniometer head, and positioned on the CAD-4 diffractometer. The solution was refined isotropically, following which difference Fourier maps wer employed to locate the positions of all the hydrogen atoms except one, whose location was calculated. The hydrogen atoms were then added to the solution with the isotropic thermal parameters of their parent carbons. The final full-matrix anisotropic least-squares refinement of positional and thermal parameters for all non-hydrogen atoms included 2015 observed reflections; 235 variable parameters converged to give disagreement factors R = 4.5% and R_w = 5.1%. The weighting scheme employed was $\sum_h w(|F_o| - |F_c|)^2$, where $w^{-1} = \sigma F_o$. A complete summary of experimental conditions is presented in Table VIII, and selected bond distances and angles are listed in Table IX. An ORTEP structure is presented in Figure 4.

Results and Discussion

Syntheses of the Compounds LM(CO)$_3$ (L = Tp, Tp*, Tp'; M = Cr, Mo). These compounds were readily synthesized in a two-step procedure involving initial substitution of three CO groups of the corresponding metal hexacarbonyl, followed by single-electron oxidation of the resulting tris(pyrazolyl)borate metal tricarbonyl complex, i.e.

$$M(CO)_6 + NaTp \xrightarrow{Et_4NCl} Et_4N[TpM(CO)_3] + NaCl \quad (1)$$

$$Et_4N[TpM(CO)_3] + [Cp_2Fe]PF_6 \rightarrow TpM(CO)_3 + Cp_2Fe + Et_4NPF_6 \quad (2)$$

Table VIII. Crystallographic Data for $TpMo(CO)_3CH_2CN$

mol formula	$C_{14}H_{12}BMoN_7O_3$
mol wt	433.05
space group	$P\bar{1}$ (No. 2)
a (Å)	9.358(2)
b (Å)	10.121(2)
c (Å)	10.328(4)
α (deg)	110.81(3)
β (deg)	93.17(3)
γ (deg)	105.14(2)
vol (Å^3)	870.70
Z	2
μ (mm^{-1})	0.775
dens (g cm^{-1})	1.652
T (K)	292
cryst dimens (mm)	0.15 × 0.30 × 0.35
$F(000)$	432
λ(Mo Kα) (Å)	0.710 732
2θ range scanned (deg)	1.0 → 50.0
$(\sin\theta)/\lambda$ max	0.595
h,k,l range obsd	−11 → 11, −12 → 12, 0 → 12
no. of unique reflns	3039
no. of obsd reflns	2015 ($I > 3\sigma_I$)

Table IX. Selected Bond Lengths and Angles of $TpMo(CO)_3CH_2CN$

	Bond Lengths (Å)		
Mo–N11	2.251(6)	C1–O1	1.147(9)
Mo–N21	2.241(5)	C2–O2	1.13(1)
Mo–N31	2.294(4)	C3–O3	1.16(1)
Mo–C1	1.971(7)	C4–C5	1.41(1)
Mo–C2	1.972(8)	C5–N5	1.13(1)
Mo–C3	1.948(8)		
Mo–C4	2.323(5)		
	Bond Angles (deg)		
N11–Mo–C1	80.7(3)	C1–Mo–C2	103.7(3)
N11–Mo–C2	164.0(2)	C1–Mo–C3	70.6(3)
N11–Mo–C3	122.7(3)	C1–Mo–C4	70.5(2)
N11–Mo–C4	89.6(2)	C2–Mo–C3	73.0(3)
N21–Mo–C1	148.1(2)	C2–Mo–C4	77.7(2)
N21–Mo–C2	86.4(3)	C3–Mo–C4	123.0(3)
N21–Mo–C3	140.8(3)	Mo–C1–O1	175.5(6)
N21–Mo–C4	82.6(2)	Mo–C2–O2	179.7(5)
N31–Mo–C1	125.0(2)	Mo–C3–O3	175.4(7)
N31–Mo–C2	107.8(2)	Mo–C4–C5	122.1(5)
N31–Mo–C3	77.2(2)	C4–C5–N5	178.3(6)
N31–Mo–C4	159.4(2)	N11–Mo–N21	82.3(2)
N11–Mo–N31	80.9(2)	N21–Mo–N31	78.1(2)

Although $TpMo(CO)_3$[5a,b] is thermally stable at room temperature, the chromium analogue is too labile to be obtained pure and was identified on the basis of comparisons of IR and NMR spectroscopic data with those of stable chromium and molybdenum analogues (Tables I and II). Besides the previously reported $TpMo(CO)_3$ and $Tp^*Mo(CO)_3$, the ligand-substituted derivatives $Tp^*Cr(CO)_3$ and $Tp'Cr(CO)_3$ are sufficiently stable that they may be isolated analytically pure. In addition, the X-ray crystal structure of the latter has been determined and compared with that of the 18-electron, manganese analogue (see below).

As can be seen from Table I, the carbonyl stretching frequencies of all of the 17-electron compounds of chromium and molybdenum are similar, and are about 100 cm^{-1} higher in frequency than the carbonyl stretching frequencies of the corresponding 18-electron anions. In addition, the carbonyl stretching frequencies of the 17-electron compounds $TpCr(CO)_3$ and $Tp'Cr(CO)_3$ are lower than those of the 18-electron, neutral manganese analogues, presumably because of decreased back-donation to the carbonyl groups of the latter species.

The new compounds were also characterized by their EPR spectra. As indicated previously,[6] the compound

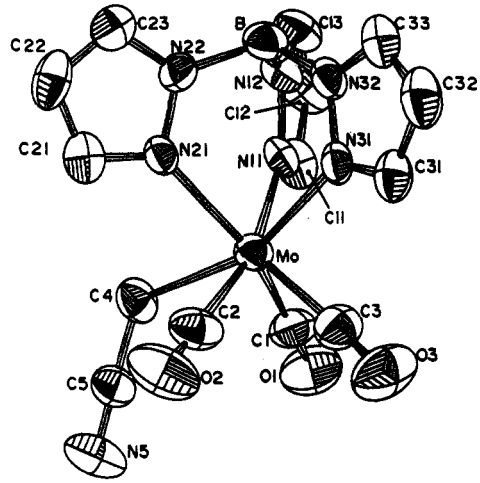

Figure 4. ORTEP plot of $TpMo(CO)_3CH_2CN$.

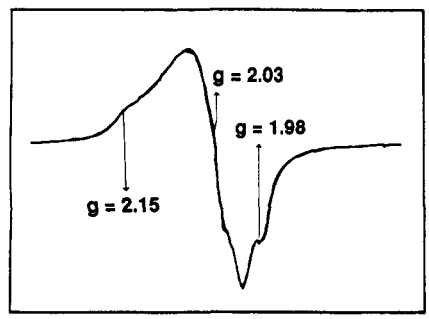

Figure 5. First-derivative EPR spectrum of $TpCr(CO)_3$ in frozen CH_2Cl_2 at 5 K.

$TpMo(CO)_3$ is EPR silent in the solid state, even to temperatures as low as 5 K, because of efficient electronic relaxation arising from the near orbital degeneracy which results from the essentially C_{3v} structure in the solid state. However, as illustrated for $TpCr(CO)_3$ in Figure 5, the compounds $TpCr(CO)_3$, $Tp^*Cr(CO)_3$, $TpMo(CO)_3$, and $Tp^*Mo(CO)_3$ all exhibit similar, broad, powderlike EPR spectra[6] in frozen methylene chloride solutions at 5 K; these spectra may be interpreted in terms of a rhombic **g** matrix. EPR spectra are not, however, detectable in frozen solutions above 77 K, and it appears that the lower site symmetries offered by the glassy solvent matricies at 5 K split the degeneracies sufficiently to permit observation of spectra. At higher temperatures, motions within the solids effectively restore the degeneracies and broaden the spectra beyond detection.

The subtlety of the dynamic Jahn–Teller distortion, which seems to account for the complete undetectability of $TpMo(CO)_3$ in single-crystal EPR work and to be responsible for the difficulties in obtaining good frozen solution EPR spectra of $TpM(CO)_3$ and $Tp^*M(CO)_3$ (M = Mo, Cr), seemed to call for a more careful approach to the challenge of symmetry reduction. To meet this challenge, we chose to synthesize an asymmetric Tp ligand which would retain the gross electronic properties of the symmetric species heretofore employed.

The known ligand $[B(Pz)_4]^-$ (Tp')[11a] possesses only C_s symmetry in the limiting case where the fourth pyrazole is restricted from free rotation. Thus, in the solid state at least, the resultant $Tp'Mo(CO)_3$ would have overall C_s symmetry (or lower) while the geometry and bonding at the metal center would be virtually identical to the parent $TpMo(CO)_3$.[5b] This seemed to provide an ideal challenge of the original hypothesis: if symmetry constraints were

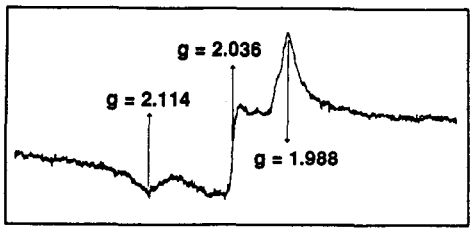

Figure 6. First-derivative EPR spectrum of $Tp'Cr(CO)_3$ in frozen hexane at 120 K.

responsible for the anomalous EPR results of $TpMo(CO)_3$, then eliminating these constraints without significantly perturbing the structure at the metal atom should still afford more readily detectable EPR signals.

EPR spectra of both $Tp'Mo(CO)_3$ and $Tp'Cr(CO)_3$ were originally measured in frozen CH_2Cl_2 and hexane solutions at 77 K. The molybdenum species was detectable but its spectrum was very broad at that temperature, while the spectrum of the chromium species was reasonably well resolved. A brief variable temperature EPR study of $Tp'Cr(CO)_3$ was carried out, with spectra being recorded in the solid state up to 150 K. The rhombic spectrum of $Tp'Cr(CO)_3$ at 120 K in frozen hexane is presented in Figure 6 (g_1 = 2.114, g_2 = 2.036, g_3 = 1.988, g_{av} = 2.046). Both compounds were also examined in liquid solution, but no EPR spectra could be detected down to the freezing point of either solvent. Upon freezing however, the $Tp'Cr(CO)_3$ signal could be detected in both CH_2Cl_2 and hexanes. The temperature limit for detection of $Tp'Mo(CO)_3$ was not accurately determined.

The explanation of the variable temperature behavior documented for $Tp'Cr(CO)_3$ was consistent with the symmetry constraints originally postulated to accompany the Tp′ ligand. If the unbound pyrazole group capping the boron atom experiences free rotation, then the overall averaged C_{3v} symmetry would render the EPR spectrum undetectable. When the solution was frozen, this free rotation would become hindered, lowering the symmetry and allowing a spectrum to be recorded. A similar mechanism is likely active for the molybdenum compound as well, although the greater g shifts broaden the spectrum and require somewhat lower temperatures to permit it to be observed.

Phosphine-Substitution Reactions. Phosphine-substitution reactions of the 17-electron tricarbonylchromium compounds were found to proceed more slowly than those of their molybdenum analogues, but the final products were often more stable. Even the smallest phosphine in the series, PMe_3, present in excess, required a full 24 h at room temperature to react to completion with $TpCr(CO)_3$. The substituted compound $TpCr(CO)_2(PMe_3)$ was characterized by elemental analyses and IR and EPR spectroscopy, but not by ^1H NMR spectroscopy. We have found that ^1H NMR spectra are unobtainable for any of the phosphine-substituted, 17-electron compounds under consideration here; presumably, the resonances are undetectably broad because of very short ^1H spin–lattice relaxation times, a conclusion consistent with the generally well resolved solution phase EPR spectra.[13]

The EPR spectrum of $TpCr(CO)_2PMe_3$ in CH_2Cl_2 solution exhibited a doublet, with hyperfine coupling to one ^{31}P nucleus, even in liquid solution. A spectrum at

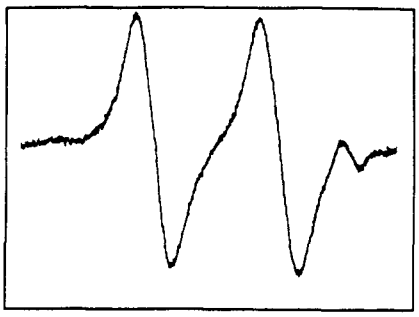

Figure 7. First-derivative EPR structure of $TpCr(CO)_2PMe_3$ in CH_2Cl_2 at 225 K.

225 K was well resolved, with g_{iso} = 2.0235 and $a(^{31}P)$ = 33.5 G (95 MHz). The experimental spectrum is reproduced in Figure 7. The spectral data are comparable with data previously reported from single crystal studies of $CpCr(CO)_2PPh_3$[3f] (g_{av} = 2.0388 and $a(^{31}P)$ = 95 MHz) and $Cp^*Cr(CO)_2PMe_3$[3f] (g_{av} = 2.0376 and $a(^{31}P)$ = 109 MHz). A substantial reduction of the isotropic g shift on substitution of CO by tertiary phosphines is noted for both series of 17-electron compounds.

Substitution of $TpCr(CO)_3$ with PMe_2Ph was slower than with PMe_3; the product, $TpCr(CO)_2(PMe_2Ph)$, was characterized only by IR spectroscopy. Substitution of $TpCr'(CO)_3$ with PBu_3 proceeded rather more smoothly, and the product, $Tp'Cr(CO)_2(PBu_3)$, was also identified by its IR spectrum.

Substitution reactions of $TpMo(CO)_3$ with the small phosphines PMe_3 (cone angle[14] 116°) and PMe_2Ph (cone angle 122°) proceeded quickly, reaching completion in less than 1 h even when cooled to 233 K. The slightly larger ligands $PMePh_2$ and PEt_2Ph (cone angles 136°) required approximately 3 h at room temperature to react completely, however, and $PEtPh_2$ (cone angle 140°) required a full 24 h. In all cases, the substituted 17-electron compounds could be readily identified on the basis of their IR spectra.

Although the ratio of $TpMo(CO)_3$ to phosphine was not constant throughout these experiments, the observed reaction times do provide qualitative comparisons of the relative ease with which the phosphines can participate in substitution reactions. The difficulties in substituting the larger phosphines indicated the relevance of steric effects in these reactions and, consistent with this conclusion, it was observed that PPh_3 did not react with $TpMo(CO)_3$. Refluxing for 2 h in THF resulted in decomposition without any evidence of substitution, and stirring the solution at room temperature with an additional 2-fold excess of Me_3NO for 48 h proved similarly fruitless. Reactions of $Tp'Mo(CO)_3$ were also carried out with PMe_3, PMe_2Ph, and PBu_3 (PBu_3 cone angle 132°); the observed rates of reaction, as determined by consumption of the initial tricarbonyl compound, were very similar to those of $TpMo(CO)_3$.

These experimental results clearly indicate a steric barrier to substitution of approximately 140° for reactions with $TpMo(CO)_3$. Although comparisons with the analogous $CpMo(CO)_3$ system are impossible, we note that monomeric compounds of the type $CpCr(CO)_2L$ have been reported with ligands as large as PCy_3[3j] (cone angle 170°). In contrast, the steric barrier of 140° determined here for $TpMo(CO)_3$ is effectively that previously reported for

(13) La Mar, G. N.; Horrocks, W. D.; Holm, R. H., Eds.; *NMR of Paramagnetic Molecules*; Academic Press: New York, 1973.

(14) Tolman, C. A. *Chem. Soc. Rev.* **1972**, *1*, 337.

$Cp^*Cr(CO)_3$,[3k] which is inert to $PMePh_2$ (cone angle 140°). Indded, parallels between the electronic properties of the $CpCr(CO)_3$ and $TpM(CO)_3$ classes of compounds have been noted previously,[15] and it has been suggested that the steric requirements of the Tp ligand are very similar to those of the bulky Cp* (η^5-C_5Me_5) ligand, the cone angles of Tp, Cp, and Cp* being estimated as 180, 100, and 146°, respectively.[5a,b]

Substitution reactions of $Tp^*Mo(CO)_3$ were examined also and, consistent with a recent report,[7b] we find that this compound reacts with neither PMe_3 nor PPh_3. Consistent with these observations, it has been previously suggested that the steric protection afforded the metal center by the Tp* ligand is sufficient to render the resultant compound air-stable, presumably by precluding approach of atmospheric oxygen.[5c]

The clear correlation between the phosphine-substitution lability and ligand cone angle for the tris(pyrazolyl)-borate compounds of chromium and molybdenum suggests that an associative mechanism is operative, as has been demonstrated previously for the compounds $CpCr(CO)_3$ and $Cp^*Cr(CO)_3$.[3k] The greater reactivity of $TpMo(CO)_3$ than its chromium analogue is likely a combination of both steric and electronic effects. The smaller radial extension of the 3d orbitals of the chromium species requires closer approach of the ligands to achieve effective bonding. Specific evidence for this is available from the X-ray crystallographic data of $Tp'Cr(CO)_3$ and $TpMo(CO)_3$; the average N–Cr bond length is 0.13 Å shorter than the corresponding average N–Mo bond length. A similar result is obtained from the metal carbonyl distances, where the difference in average bond lengths is 0.12 Å. Since closer ligand approach to the chromium would be required to obtain the stabilization of the 3e 2c intermediate, the repulsive influences of the steric factors with the smaller metal atom would be further exacerbated.

The importance of an associative ligand-substitution process may also be affected by the electron density at the metal center. It has been reported that formation of $V(CO)_4(PBu_3)_2$ from the monosubstituted species is almost 10^5 slower than is substitution of the hexacarbonyl parent;[16] while steric effects are undoubtedly important, it has been suggested that the greater electron density on the metal center due to the presence of a phosphine ligand may also reduce the susceptibility of the monosubstituted compound to further reaction.[16] The results of the electrochemical experiments, reported below, clearly demonstrate that reduction of $TpCr(CO)_3$ required 0.2 V more than that of $TpMo(CO)_3$, and hence that the chromium species might be anticipated to be less prone to stabilize a 19-electron intermediate, regardless of steric factors.

As noted above, interesting byproducts were observed during several of the phosphine-substitution experiments. For instance, formation of the hydride, $TpMo(CO)_3H$,[5] was found to occur during substitution experiments of $TpMo(CO)_3$ with the larger phosphines. The hydride is, however, a normal product of thermal decomposition of $TpMo(CO)_3$ and presumably forms because substitution rates of the larger phosphines are sufficiently slow that $TpMo(CO)_3$ remains in solution long enough for decomposition to occur.

An unanticipated result of the substitution chemistry was the apparent formation of several phosphine-substituted hydride compounds, $TpMo(CO)_2(PMe_2Ph)H$, $Tp'Mo(CO)_2(PMe_3)H$, and $Tp'Mo(CO)_2(PBu_3)H$. Although these hydrides were formed in sufficiently small quantities that they could not be isolated pure, their identification on the basis of IR and NMR spectroscopic evidence seems firm. Control experiments, in which $Tp'Mo(CO)_3H$ and $[NEt_4][Tp'Mo(CO)_3]$ were reacted with PMe_3, did not result in the formation of $Tp'Mo(CO)_2(PMe_3)H$, and thus it would seem that his hydride results from thermal decomposition of $Tp'Mo(CO)_2(PMe_3)$. The source of the hydride ligands is not known.

During many of the substitution reactions, high frequency IR bands were observed near 2040 and 1964 cm^{-1}. While these peaks were initially very strong but grew rapidly weaker in intensity during the reactions of $TpMo(CO)_3$ with PMe_3 and PMe_2Ph, they were still present after 3 h during reaction of PEt_2Ph, were not observed during substitution reactions of $TpCr(CO)_3$, and were relatively weak during reaction of $TpMo(CO)_3$ with PBu_3 in toluene.

The frequencies of these bands are very similar to those of the complexes $TpMo(CO)_3Br$[12] (2043 and 1968 cm^{-1} in CH_2Cl_2) and $[Tp^*W(CO)_3(CH_3CN)]^+$ (2045 and 1955 cm^{-1}),[17] suggesting that the species giving rise to the high frequency bands are in the +2 oxidation state and result from disproportionation processes accompanying ligand substitutions (eq 3).

$$2TpMo(CO)_3 + L \rightarrow [TpMo(CO)_3L][TpMo(CO)_3] \quad (3)$$

In agreement with this hypothesis, IR bands attributable to $[TpMo(CO)_3]^-$ were observed as low frequency shoulders on the peaks of the phosphine-substituted compounds in, for instance, the reactions of $TpMo(CO)_3$ with PMe_3 and PMe_2Ph. These observations are consistent with a previous report describing the phosphine-substitution chemistry of $CpCr(CO)_3$,[3k] during which phosphine ligands were observed to react to form complexes of the type $[CpCr(CO)_2L_2][CpCr(CO)_3]$. As well, reactions conducted in THF generated greater ratios of disproportionation products to substitution products than when the reactions were duplicated in the less polar solvent toluene.

X-ray Crystal Structures of $Tp'Cr(CO)_3$, $Tp'Mn(CO)_3$, and $TpMo(CO)_2(PEt_2Ph)$. The crystal structures of $Tp'Cr(CO)_3$ and, for purposes of comparison, $Tp'Mn(CO)_3$ were determined; selected bond lengths and angles for both are listed in Table IV, while ORTEP plots are presented in Figures 1 and 3.

The structures of both Tp' ligands are unremarkable, being very similar and closely resembling the structure of the Tp ligand of $TpMo(CO)_3$.[5a,b] Furthermore, the orientations of the uncoordinated pyrazole rings are similar in the two structures, in both cases being approximately parallel to the OC(1) carbonyl groups. The generally longer Cr–ligand bond lengths presumably reflect the anticipated larger chromium covalent radius; the observed bond distances in both complexes correlate well with comparable examples recorded in the Cambridge Crystallograhic Database.[18]

Of special structural interest is the pronounced distortion of the OC–Cr–Co bond angles of $Tp'Cr(CO)_3$ relative

(15) Trofimenko, S. *Acc. Chem. Res.* **1971**, *4*, 17.
(16) Shi, Q-Z.; Richmond, T. G.; Trogler, W. C.; Basolo, F. *J. Am. Chem. Soc.* **1984**, *106*, 71.
(17) Feng, S. G.; Phillip, C. C.; White, P. S.; Templeton, J. L. *Organometallics* **1991**, *10*, 3504.
(18) Orpen, G. A.; Brammer, L.; Allen, F. H.; Kennard, O.; Watson, D. G.; Taylor, R. *J. Chem. Soc., Dalton Trans.* **1989**, S1.

Table X. Reduction Potentials for the $LM(CO)_2L'$/$LM(CO)_2L'$ Couples (L' = CO, Tertiary Phosphines)

compd	$E°(CH_2Cl_2)$ (V)	$E°(CH_3CN)$ (V)
$TpCr(CO)_3$	−0.17	−0.16
$Tp*Cr(CO)_3$	−0.14	−0.08
$Tp'Cr(CO)_3$	−0.16	−0.08
$TpMo(CO)_3$	−0.02	+0.09
$Tp*Mo(CO)_3$	−0.05	+0.02
$Tp'Mo(CO)_3$	0.00	+0.08
$TpCr(CO)_2(PMe_3)$	−0.87[a]	
$TpCr(CO)_2(PMe_2Ph)$	−0.81[a]	
$TpMo(CO)_2(PMe_2Ph)$	−0.55[a]	

[a] In THF.

to the approximately 90° bond angles of the 18-electron analogue, $Tp'Mn(CO)_3$. As can be seen, the OC(2)–Cr–OC(3) bond angle is significantly greater than 90°, the other OC–Cr–OC bond angles being reduced accordingly. While the structure of $Tp'Cr(CO)_3$ thus differs significantly from that of $TpMo(CO)_3$,[5a,b] which assumes essentially the idealized C_{3v} structure of $TpMn(CO)_3$, the pattern of OC–M–OC bond angles is very similar to that of $Tp*Mo(CO)_3$,[7d] to those of both conformers of $(\eta^5\text{-}C_5Ph_5)Cr(CO)_3$,[3i] and to that of the structure predicted theoretically for the monomer, $CpCr(CO)_3$.[3f] Thus the results appear to provide evidence in support of the earlier theoretical predictions; indeed, it appears that the potential energy surface for OC–M–OC bending in these molecules is very flat,[3f] and thus the relatively high symmetry of $TpMo(CO)_3$[5a,b] may be fortuitous.

The X-ray crystal structure of the phosphine-substituted compound $TpMo(CO)_2(PEt_2Ph)$ was also determined (Figure 2). Again the geometry of the Tp ligand was essentially as anticipated, and the most interesting observation is that the OC–Mo–CO angle has contracted from the approximately 90° angles of $TpMo(CO)_3$ and most 18-electron species[3a,f] to an angle of 80.0(1)°. This bond angle is very similar to the OC–Cr–CO angles of 80.9(1)° in $CpCr(CO)_2(PPh_3)$[3a,f] and 79.7(3)° in $Cp*Cr(CO)_2(PMe_3)$,[3a,f] although no clear plane of symmetry exists in the structure of $TpMo(CO)_2(PEt_2Ph)$ and the OC–Mo–CO bond angle distortions do not occur symmetrically but are reflected instead in substantial deviation of the C(2) carbonyl group. As shown in Table VI, the P–Mo–C(1) bond angle is close to 90° while the P–Mo–C(2) bond angle is opened substantially, to greater than 97°. The ORTEP plot of $TpMo(CO)_2(PEt_2Ph)$ shows that the phenyl group on the phosphine occupies a position adjacent to the C(2) carbonyl group, and its steric requirements may also be a factor in the OC–Mo–CO contraction observed for this compound.

Electrochemical Properties. Cyclic voltammagrams of the compounds $[NEt_4][LM(CO)_3]$ and $LM(CO)_3$ (L = Tp, Tp*, Tp'; M = Mo, Cr) were recorded in CH_2Cl_2 and acetonitrile solutions, CV spectra of ferrocene being used for calibration purposes.[9] Identical CVs were obtained whether beginning with anionic or neutral species, in all cases quasi-reversible CVs being obtained with current ratios I_{red}/I_{ox} typically in the range 0.75–0.90 and with ΔE ($E°_{ox} - E°_{red}$) values slightly larger than those observed for the ferrocene reference in each solvent. The $E°$ values reported in Table X are the averages of the recorded $E°_{ox}$ and $E°_{red}$ values obtained from the CV plots. Comparison of the current responses observed in the CV spectra of the anions with those recorded for an equivalent concentration of ferrocene showed that 1-electron transfers were occurring in all samples, as depicted in eq 4. The reduction

$$LM(CO)_3 + e^- \rightleftarrows [LM(CO)_3]^- \quad (4)$$

potentials observed are very similar to those of $CpCr(CO)_3$ (−0.10 V) and $Cp*Cr(CO)_3$ (−0.24 V) in CH_2Cl_2.[3h] Irreversible oxidation waves were also observed to more positive potentials in each case, but were not investigated further; typical examples of experimental CV scans are presented in Figure 8.

We have also investigated electrochemical properties of the phosphine-substituted compounds $TpCr(CO)_2(PMe_3)$, $TpCr(CO)_2(PMe_2Ph)$, and $TpMo(CO)_2(PMePh_2)$. The CV of each of these displays a quasi-reversible reduction wave and two irreversible oxidation waves, as shown in Figure 8; the experimentally determined reduction potentials are listed in Table X. As can be seen, the 1-electron reduction potentials of the substituted compounds are approximately 0.5 V more negative than the corresponding potentials of the tricarbonyl compounds, consistent with the anticipated higher electron densities in the former. Similar correlations have been observed for 1-electron reductions of compounds of the type $CpCr(CO)_2L$ (L = CO, tertiary phosphines).[3h]

While this investigation was in progress, there appeared two reports in which the electrochemistry of the $[Tp*M(CO)_3]^-/Tp*M(CO)_3$ couple was explored.[7b,c] While details of the results of these investigations differ from ours, presumably because of somewhat different experimental conditions, the trends observed are in very good agreement with those observed by us.

Synthesis and Structure of $TpMo(CO)_3CH_2CN$. Reactions of bromoacetonitrile with $TpMo(CO)_3$ and $TpMo(CO)_3^-$ both result in the rapid formation of $TpMo(CO)_3CH_2CN$ (eqs 5 and 6). The compound is the

$$TpMo(CO)_3 + BrCH_2CN \rightarrow TpMo(CO)_3CH_2CN + TpMo(CO)_3Br \quad (5)$$

$$TpMo(CO)_3^- + BrCH_2CN \rightarrow TpMo(CO)_3CH_2CN + Br^- \quad (6)$$

first well-characterized example of an alkyl compound of the type $TpM(CO)_3R$ and is sufficiently stable to be purified and recrystallized. It was unambiguously characterized by elemental analyses, IR and NMR spectroscopy, and X-ray crystallography and by its formation from the reaction of bromoacetonitrile with $[NEt_4][TpMo(CO)_3]$. The IR spectrum of this compound exhibits $\nu(CO)$ at 2025 (s), 1942 (s), and 1927 cm^{-1} (m, sh) in CH_2Cl_2, at 2024 (s), 1944 (s), and 1921 cm^{-1} (m) in toluene.

The chemistry of eq 5 presumably involves bromine atom abstraction reaction, followed by coupling of the resulting alkyl radical with a second molecule of $TpMo(CO)_3$ (eqs 7 and 8). A similar sequence of reactions has

$$TpMo(CO)_3 + BrCH_2CN \rightarrow TpMo(CO)_3Br + {}^{\bullet}CH_2CN \quad (7)$$

$$TpMo(CO)_3 + {}^{\bullet}CH_2CN \rightarrow TpMo(CO)_3CH_2CN \quad (8)$$

been postulated for analogous reactions of $CpCr(CO)_3$ with alkyl halides.[3l] However, in contrast to the cyclopenta-

(19) Chaiwasie, S.; Fenn, R. H. *Acta Crystallogr., Sect. B* **1968**, *B24*, 525.

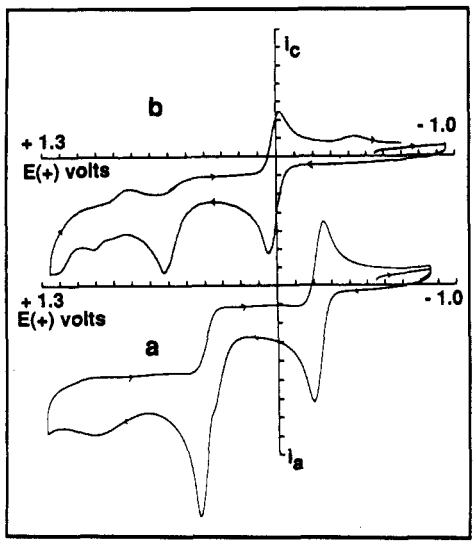

Figure 8. Cyclic voltammograms of the $TpCr(CO)_3$/$TpCr(CO)_3^-$ (a) and $TpMo(CO)_3$/$TpMo(CO)_3^-$ (b) couples.

dienylchromium system, which reacts with a wide variety of alkyl halides, $TpMo(CO)_3$ was found to be relatively inert, even to those alkyl halides which react readily with $CpCr(CO)_3$. It is possible that steric considerations are important in deactivating the Tp system in this way.

The structure of $TpMo(CO)_3CH_2CN$ is shown in Figure 4; bond lengths and angles are in Table IX. As can be seen, the compound assumes a "four-legged piano stool" or 3:4 structure, similar to that of $TpMo(CO)_3Br$[12] and common for compounds of the type $CpML_4$. As with $TpMo(CO)_3Br$, the mutually "trans" Mo–CO bonds are longer than the unique Mo–CO bond and the "trans" OC–Mo–Co bond angle is larger than the X–Mo–CO (X = Br, CH_2CN) bond angle. However, the Mo–N bond lengths of $TpMo(CO)_3CH_2CN$ are all slightly longer than the corresponding bonds of $TpMo(CO)_3Br$, the Mo–CO bond lengths slightly shorter. In addition, we note that the average values of the Mo–CO bond lengths of $TpMo(CO)_3CH_2CN$ are 0.08 Å longer than those previously determined for $TpMo(CO)_2(PEt_2Ph)$,[5] consistent with the formal +2 oxidation state and hence weaker back-bonding in the former. Finally, we note that the trans OC–Mo–CH_2CN bond angle, 123.0(3)° and the two cis OC–Mo–CH_2CN bond angles (74.1° average) in $TpMo(CO)_3CH_2CN$ are smaller than the corresponding angles of $CpMo(CO)_3Cl$,[19] $CpMo(CO)_3CH_2CO_2H$,[20] and $CpMo(CO)_3CF_2CF_2CF_3$[21] (averages 134 and 76.7°, respectively).

Acknowledgment. The Natural Sciences and Engineering Council of Canada is thanked for an Operating Grant to M.C.B. and a Graduate Fellowship to J.H.M. We thank also Professor Mats Tilset for a preprint of ref 7c and Professor J. A. Page for helpful discussions.

Supplementary Material Available: For $Tp'Cr(CO)_3$, $Tp'Mn(CO)_3$, $TpMo(CO)_2(PEt_2Ph)$, and $TpMo(CO)_3CH_2CN$, tables of positional and isotropic thermal parameters, anisotropic thermal parameters, and bond lengths and angles (17 pages). Ordering information is given on any current masthead page.

OM930611I

(20) Ariyatne, J. K. P.; Bjerrum, A. M.; Green, M. L. H.; Ishaq, M.; Prout, C. K.; Swanwick, M. G. *J. Chem. Soc. A* **1969**, 1309.
(21) Churchill, M. R.; Fennessey, J. P. *Inorg. Chem.* **1967**, *6*, 1213.